AEGC Australasian Exploration Geoscience Conference Brisbane 2021

Predicting fluid pathways in large discontinuity systems using graph theory

Ulrich Kelka
CSIRO Mineral Resources
Kensington, WA 6151
Uli.kelka@csiro.au

Stefan Westerlund
CSIRO Data61
Kensington, WA 6151
Stefan.Westerlund@csiro.au

Thomas Poulet
CSIRO Mineral Resources
Kensington, WA 6151
Thomas.Poulet@csiro.au

Luk Peeters
CSIRO Land & Water
Adelaide SA 5064
Luk.Peeters@csiro.au

SUMMARY

Fracture networks and fault zones play an important role for subsurface fluid flow. Estimating the impact on the permeability field of such structures is of high interest for reservoir characterization, groundwater management, and exploration targeting. Of particular interest is the anisotropic permeability resulting from fracture sets, which can be represented as a tensor. These permeabilities of small- to mesoscale fracture networks can be utilized in macroscale models of macroscale fault networks. Obtaining exact permeability values from fractured rocks through laboratory experiments is challenging and subject to large uncertainties. Numerical methods can help estimating reliable values but are computationally expensive.

On the large scale it is desirable to predict the dominant pathways in fault networks as these zones can strongly affect localization of mineralizing fluids, can affect the productivity of reservoirs (hydrocarbon and geothermal), and has implications for groundwater management.

Here, we present a methodology that (1) allows for estimating permeability anisotropy, and (2) predicting dominant fluid pathways from regional scale maps. Assuming that the permeability of fractured or faulted media is governed by the connectivity of the network entities, we will show how permeability anisotropy and dominant pathways can be obtained from a graph representation of 2D discontinuity networks. The graph metrics we base our analysis on are the betweenness centrality and maximum flow.

Key words: fault zones, fracture networks, graph theory

INTRODUCTION

Densities, orientation, and connectivity of fault and fractures exhibit a strong influence on permeability resulting in anisotropic flow fields. Discontinuity networks that are the result of numerous subsequent deformation events are likely to exhibit a strong anisotropy and characterizing this with laboratory experiments is challenging and cost intensive. Solving flow on unit cubes in numerical simulations is one way for capturing the anisotropy of discontinuity networks and represents a homogenization method that allows for combining discontinuity networks of different scales in large scale models. An example is a network of fault zones hosted in low porosity rocks. The background permeability of the host-rock will be a function of the fracture abundance that increases in the fault zones with highest fracture densities in zones adjacent to fault cores.

The parameter comprising the highest uncertainties are the apertures of the fractures that also affects the permeability distribution within the fault zones. Numerous hydraulic simulations would have to be conducted to capture the distributions of possible permeability tensors at the smaller scales around the faults and investigate their impact in the large-scale models.

In this contribution, we present a methodology for obtaining the shape of the anisotropy tensor that can be used for upscaling the smaller scale network permeability to a continuum model. In addition, we will show how to determine the connected components and dominant pathways in large-scale fault networks, which is of interest for targeting by identifying structures that are crucial for fluid flow in hydrothermal systems that form economic mineralization.

We will show the applicability of our framework on a fracture network from the Bristol Channel, UK, and on structural interpretation of an area in the Central Gawler Craton in South Australia (figure 1).

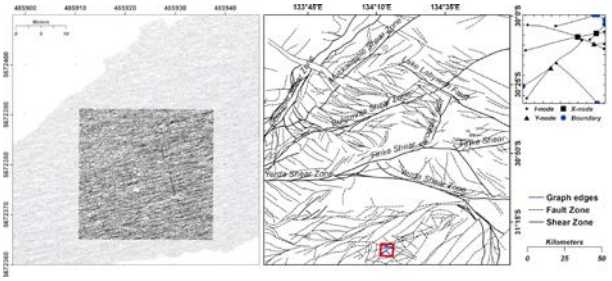

Figure 1: Left: High detail fracture network in the Bristol channel, UK automatically mapped from drone imaginary (Prabhakaran et al., 2021). The features contained in the rectangular area represent the dataset analysed in this study (~2400 fractures). Right: Fault zone network located in the Central Gawler Craton of South Australia. The high-resolution total magnetic intensity map (Katona et al., 2019) was the basis for manually performing the structural interpretation (courtesy Mark Pawley). The fault traces contained by the red rectangle are shown in the upper right, visualizing how we build a 2D referenced graph. Fault segments are the edges whereas tips and intersection points are considered as the vertices. The degree of a vertex (number of edges meeting at this point) is used to classify the intersections as either *Y*- (degree of 3) or *X*-vertices (degree of 4). Fault or fracture tips that have a degree of 1 are classified as *I*-nodes. Note that vertices that are located at intersections with the bounding box of the area of interest are classified as boundary nodes (blue vertices) and will be connected to virtual source and target nodes for solving the maximum flow.

METHODS

We base our analysis on 2D trace maps of discontinuities that are provided as vector data. The first step is to correct for digitization flaws in the data. The common defects are

duplicated entries, incorrectly split traces, or traces that are not clipped to other traces which can lead to false classification of intersections (e.g. crossing instead of junction). In figure 1 we show the two datasets we investigate and introduce the graph data structure we use in the analysis. In the following we brief the graph algorithms we applied.

Betweenness Centrality

Centrality (*C*) is a measure of the importance of a vertex in the network for maintaining connectivity. We utilize the Brandes' betweenness centrality of the BOOST graph library (Siek et al., 2002) which is a measure of how many shortest paths between randomly chosen vertices *s* and *t* pass through a vertex(*v*) in the network. The absolute betweenness centrality is defined as:

$$C(v) = \sum_{s \neq v \neq t} \frac{\sigma_{st}(v)}{\sigma_{st}} \quad (1)$$

Here σ_{st} is the number of shortest paths between source (*s*) and target (*t*) and $\sigma_{st}(v)$ is the number of shortest paths through the vertex *v*.

Maximum Flow

Maximum flow analysis determines the maximum possible flow rate in a directed graph between a source (*s*) and target (*t*) vertex. We choose BOOST's implementation of *Boykov-Kolmogorov* maximum flow (Siek et al., 2002) as this network flow algorithm was shown to be applicable to flow in pipe and river networks (Zhou et al., 2020).

Maximum flow is solved on a directed graph *G=(V,E)* comprising a single source (*s*) and target (*t*) vertex. Each edge has a positive capacity (*C*) proportional to the amount of flow that can pass through this edge. A function must be defined for the flow that can pass though the edge from the adjacent vertices. This function (*f*) must satisfy three conditions (Siek et al., 2002):

$$f\ (u,v) \leq c(u.v)\ \forall\ (u,v)\ in\ VxV \quad (2)$$
$$f(u,v) = -f(u,v)\ \forall\ (u,v) in\ VxV \quad (3)$$
$$\sum_{v\ in\ V} f(u,v) = 0\ \forall\ u\ in\ V - \{s,t\} \quad (4)$$

The maximum flow represents the path through a network comprising the maximum sum of capacities between the source and the target with:

$$|f| = \sum_{u\ in\ V} f(u,t) = \sum_{v\ in\ V} f(s,v) \quad (5)$$

In our approach to the maximum flow problem we first determine the model boundaries by constructing a rectangular envelope around the line features. We then shrink this rectangle by a defined percentage to ensure intersections between features and boundaries. At every intersection a new vertex is inserted and connected to a virtual vertex outside the domain by an edge of infinite capacity. A constant gradient (*p)* from 0 and 1 is calculated between two opposing boundaries and every vertex will have a value of *p* assigned to it. Based on the values of *p* assigned to the vertices, we define an additional constraint for the capacity at edge (*i*) pointing from vertex *u* to vertex *v* that considers the gradient of $\Delta p = p_u - p_v$ over the length of the edge (l_{uv}):

$$C = C_i \cdot \frac{\Delta p}{l_{uv}} \quad (6)$$

We define three types of capacities that are shown in table 1. Type 1 determines the edge capacity as the square root of its length accounting for the scaling relationships between aperture size and length in a fracture or the scaling between displacements and length of faults. The latter enhances the permeability of fault zones in low-porosity rocks via fracturing. The capacity type 2 is a function of edge orientation (α) with capacity values derived from a Gaussian distribution around a mean angle (μ) with a standard deviation (σ) of 25°. This capacity accounts for the relation between apertures and maximum stress orientation where fractures perpendicular to the maximum compression are closing resulting in a permeability reduction. Capacity type 3 combines the scaling of length and orientation dependency in single capacity. Note that all capacity values are normalized by the maximum capacity.

Investigating which edge capacities are filled, allows for predicting the dominant pathways in a network. Furthermore, performing experiments with varying conditions (e.g. gradient orientation, flow direction, and capacity type) enables analysing of the anisotropy of the network connectivity that govern flow.

Table 1: Capacity types (*C*) used for solving maximum flow. *L* is the length of the edge, σ is the standard deviation, and μ is the mean around an angle α. After obtaining the capacities for all edges we normalize by the maximum capacity (C_{max}) value giving the capacity at edge *n* as $C_n = \frac{C}{C_{max}}$.

Type	*Expression*
1 (length)	$C_l = \sqrt{l}$
2 (orientation)	$C_o = \frac{1}{\sigma\sqrt{2\pi}} \cdot e^{-\frac{1}{2}\left(\frac{\alpha-\mu}{\sigma}\right)^2} \cdot 1000$
3 (length-orientation)	$C_{lo} = C_l C_o$

Estimation of effective Permeabilities

The directional permeabilities (κ) of discontinuity networks can be estimated from the flow rates (*q*) obtained for varying pressure gradients (*P*) solved on a unit square through:

$$\begin{bmatrix} \kappa_{xx} & \kappa_{xy} \\ \kappa_{yx} & \kappa_{yy} \end{bmatrix} = \begin{bmatrix} q_{xx} & q_{xy} \\ q_{yx} & q_{yy} \end{bmatrix} \begin{bmatrix} \frac{1}{\Delta P_x} & 0 \\ 0 & \frac{1}{\Delta P_y} \end{bmatrix} \quad (7)$$

For symmetrical tensors the principal permeabilities and their orientations can be obtained as:

$$\kappa_{max} = \frac{\kappa_{xx}+\kappa_{yy}}{2} + \frac{\left|{}^{\kappa_{xy}}/_{sin2\alpha}\right|}{2} \quad (8)$$
$$\kappa_{min} = \frac{\kappa_{xx}+\kappa_{yy}}{2} - \frac{\left|{}^{\kappa_{xy}}/_{sin2\alpha}\right|}{2} \quad (9)$$
$$2\alpha = tan^{-1}\frac{-2\kappa_{xy}}{\kappa_{xx}-\kappa_{yy}} \quad (10)$$

We can derive the shape of the permeability tensor by solving the maximum flow in vertical and horizontal directions for a horizontal and vertical gradient respectively. This approach allows for investigating different capacity types and yields a normalized tensor that can then be used for detailed numerical investigation in macro-scale simulations.

RESULTS

The results of solving the maximum flow with length-dependant capacities in the Bristol Channel joint network is shown in figure 2 for a N-S gradient (a) and a E-W gradient (b). The flow direction in figure 2 equals the pressure direction. By solving the maximum flow for direction parallel and perpendicular to the gradient we can estimate the permeability tensor for uniform-, length-, and orientation capacities.

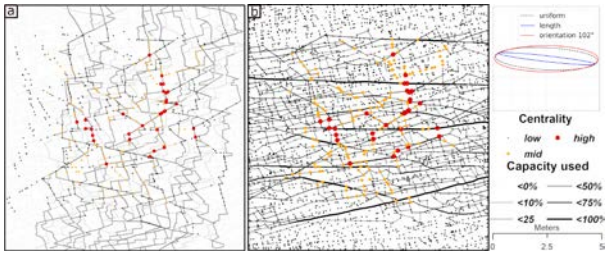

Figure 2: Maximum flow with length dependent capacities and betweenness centrality calculated on the fracture network from the Bristol channel. *a* Vertical gradient and flow. *b* Horizontal gradient and flow direction. An estimate of the permeability tensor for uniform-, length-, and orientation-capacities is shown exemplary to the upper right.

While the vertical connectivity comprises only perturbed channels that often do not have their capacity filled up (*a*), a strong connectivity exists in the horizontal direction with few straight channels extending from the right to the left boundary (*b*). The thicknesses and colouring of the edges corresponds to the proportion of the capacity filled. Comparing the dominant flow paths with the betweenness centrality of the vertices shows that there is a correlation between centrality and location of the maximum flow.

The results of length-dependant maximum flow and betweenness centrality in the Central Gawler fault networks are shown in figure 3. In this network we did not utilize a gradient constraint as this analysis does not aim at homogenizing the area but rather aims at identifying the structures that are most relevant for horizontal connectivity.

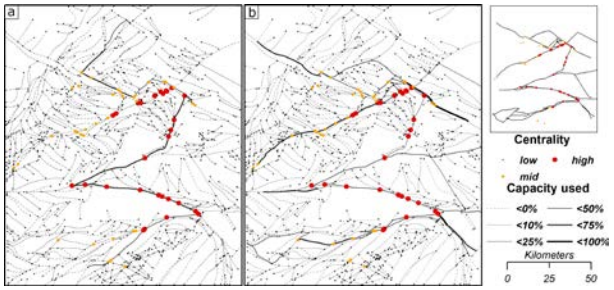

Figure 3: Maximum flow with length-dependant capacities and betweenness centrality for the structural interpretation of Gawler Craton. A dominant conduit exists in the north-south direction (a). In contrast, the connectivity in the east-west direction reveals at least three prominent channels (*b*).) Note that the connectivity for this dataset is obtained without pressure constraint (equation 6). In the upper right the edges comprising highest cumulative capacities for vertical and horizontal maximum flow and the vertex betweenness centrality is shown. This can be considered as the backbone of the regional scale fault network.

CONCLUSIONS

We have shown a simple and computationally efficient approach for estimating permeability anisotropy in fracture networks (figure 2). The results obtained can, for instance, be utilized for upscaling small scale fractures in large scale simulations where the fractured media is treated as a continuum. In the case of large-scale discontinuity networks, such as the example shown from the Central Gawler Craton in South Australia (figure 3), a homogenization of permeabilities may not feasible. Graph theory can help in this case to determine the backbone of the connectivity network (betweenness centrality) and maximum flow can be applied for determining the elements that are most important for maintaining flow though the network.

The results presented in this study will have to be evaluated by detailed numerical experiments to further demonstrate their reliability.

ACKNOWLEDGMENTS

We acknowledge CSIRO's Deep Earth Imaging Future Science Platform for supporting this research.

REFERENCES

Gaston, D., Newman, C., Hansen, G. and Lebrun-Grandié, D., 2009. MOOSE: A parallel computational framework for coupled systems of nonlinear equations: Nuclear Engineering and Design, 239, 1768 – 1778.

Geuzaine, C. and Remacle, J.-F., 2009. Gmsh: A 3-D finite element mesh generator with built-in pre- and post-processing facilities: International Journal for Numerical Methods in Engineering, 79, 1309-1331

Katona, L., Hutchens, M., and Foss, C., 2019. Geological Survey of South Australia: An overview of the Gawler Craton Airborne Survey–new data and products, Preview, 2019, 24–26, 2019.

Prabhakaran, R., Urai, J.L., Bertotti, G., C Weismüller, C., and. Smeulders D. M. J., 2021. Fracture Patterns from the Lilstock Pavement, Bristol Channel, UK https://data.4tu.nl/articles/dataset/Fracture_Patterns_from_the_Lilstock_Pavement_Bristol_Channel_UK/14039234

Siek, J., Lumsdaine, A. and Lee, L.Q., 2002. The boost graph library: user guide and reference manual. Addison-Wesley.

Zhou Y., Shi Y., Wu H., Chen Y., Yang Q., Fang Z., 2020. Evaluation Method for Water Network Connectivity Based on Graph Theory. In: Li W., Tang D. (eds) Mobile Wireless Middleware, Operating Systems and Applications. MOBILWARE 2020. Lecture Notes of the Institute for Computer Sciences, Social Informatics and Telecommunications Engineering, vol 331. Springer, Cham. https://doi.org/10.1007/978-3-030-62205-3_11